Weierstraß-Institut
für Angewandte Analysis und Stochastik
Leibniz-Institut im Forschungsverbund Berlin e. V.

Preprint ISSN 2198-5855

Analysis of an operator-differential model for magnetostrictive energy harvesting

Daniele Davino[1], Pavel Krejčí[2], Alexander Pimenov[3], Dmitrii Rachinskii[4],

Ciro Visone[1]

submitted: February 9, 2016

[1] Department of Engineering
Università del Sannio
Benevento
Italy

[2] Institute of Mathematics of
the Academy of Sciences of the Czech Republic
Prague
Czech Republic

[3] Weierstrass Institute
Mohrenstr. 39
10117 Berlin
Germany
E-Mail: alexander.pimenov@wias-berlin.de

[4] Department of Mathematical Sciences
The University of Texas at Dallas
800 W. Campbell Road
Richardson
Texas
USA

No. 2225
Berlin 2016

2010 *Mathematics Subject Classification.* 34C55, 47J40, 74F15, 37N15.

Key words and phrases. Magnetostrictive materials, hysteresis, energy harvesting, optimization problems.

P. K. acknowledges the support by GAČR Grant GA15-12227S and RVO:67985840. A. P. acknowledges the support of SFB 787 from the DFG, project B5. D. R. acknowledges the support of NSF through grant DMS-1413223. C. V. and D. D. acknowledge the support of Italian research project PON Low Noise, grant PON01-1878.

Edited by
Weierstraß-Institut für Angewandte Analysis und Stochastik (WIAS)
Leibniz-Institut im Forschungsverbund Berlin e. V.
Mohrenstraße 39
10117 Berlin
Germany

Fax: +49 30 20372-303
E-Mail: preprint@wias-berlin.de
World Wide Web: http://www.wias-berlin.de/

Abstract

We present a model of, and analysis of an optimization problem for, a magnetostrictive harvesting device which converts mechanical energy of the repetitive process such as vibrations of the smart material to electrical energy that is then supplied to an electric load. The model combines a lumped differential equation for a simple electronic circuit with an operator model for the complex constitutive law of the magnetostrictive material. The operator based on the formalism of the phenomenological Preisach model describes nonlinear saturation effects and hysteresis losses typical of magnetostrictive materials in a thermodynamically consistent fashion. We prove well-posedness of the full operator-differential system and establish global asymptotic stability of the periodic regime under periodic mechanical forcing that represents mechanical vibrations due to varying environmental conditions. Then we show the existence of an optimal solution for the problem of maximization of the output power with respect to a set of controllable parameters (for the periodically forced system). Analytical results are illustrated with numerical examples of an optimal solution.

1 Introduction

Many engineering processes imply energy conversion. Part of the energy 'released' to the environment in one or several forms, spanning from heat to vibrations, is normally considered as 'wasted'. Since the environmental (low power) energy source is everywhere available, the idea of its exploitation to supply low power devices arises naturally and leads to the concept of *Energy Harvesting*, EH [1, 2].

Energy harvesting is a technique for recovering small amounts of ambient energy, otherwise wasted, of any kind (such as light, vibrations, heat, etc.). It can be considered as a paradigm for a wiser way of energy use. In fact, EH has enabled power supply of wireless battery-free sensors and increased device efficiency through recovery and re-use of ambient energy. Design of an EH device can be based on the use of materials (usually referred to as *smart*) that demonstrate coupling between mechanical and electromagnetic properties and thus naturally perform energy conversion. Effectively, smart materials act as a natural miniature electrical generator under mechanical forcing. Thermo-electric junctions, piezoelectric, magnetostrictive and magneto-caloric materials are significant examples of smart materials that have been known for a long time. However, their exploitation for energy conversion has become possible only recently, since the development of new materials such as PZT and Terfenol-D that show a very strong coupling between mechanical and electromagnetic variables, or $SrTiO_3$ that demonstrates a giant Seebeck effect [3, 4, 5].

One of the most studied EH techniques for recovery of mechanical energy of vibrations involves alloys with strong electro- or magneto-mechanical coupling. Figure 1 presents a general schematic of a system that employs a *kinetic* energy harvesting device (harvester) to convert kinetic energy available in the form of mechanical vibrations into electrical power which is then used to feed wireless sensors. A substantial body of work has been devoted to optimization of the efficiency and maximization of the output power for such systems. Most of this work adopts a linear model for the energy conversion mechanism of the harvester and focuses on optimization of the electrical circuit of the harvester, or on careful design of the electronic circuit that

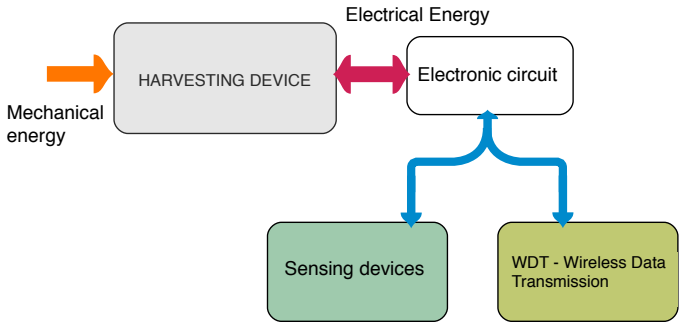

Figure 1: General scheme of a wireless sensor employing a magnetostrictive energy harvester as power source.

stores the electric energy and makes it available to sensors and data transmission modules (this electronic circuit can be considered as the *electric load* of the harvester, see Figure 1). For example, electronic techniques helping optimize the converted power of a kinetic energy harvester based on a piezoelectric element have been considered in [6]. Karush-Kuhn-Tucker (KKT) conditions have been applied to optimize the power output of a piezoelectric vibration-based energy harvester which utilizes a harvesting circuit employing an inductor and a resistive load [7]. Further analytic formulas for efficiency have been obtained from the linear theory of kinetic energy harvesting [8]. In particular, the efficiency of a mass-spring-damper system with a linear behavior of the energy converting mechanism has been considered in [9]. EH devices employing magnetostrictive materials for energy conversion have also been designed, modeled and tested as, for example, in [10] where the magnetostrictive harvester (based on metglas) is coupled with an electronic circuit to improve the conversion efficiency. Analysis presented in [10, 11] is based on a linear model of the magnetostrictive harvester.

The linear approximation and techniques based on perturbation methods are effective for modeling oscillators with relatively weak nonlinearity or sufficiently small vibrations [12]. However, all smart materials demonstrate a strongly nonlinear constitutive law. Results from piezoelectric energy harvesters [13, 14, 15, 16, 17] and preliminary results from magnetostrictive energy harvesters [18] show that nonlinearities in the material characteristic need to be accounted for in order to maximize, or significantly increase, the energy output of these devices. From a philosophical point of view, linear models displaying Onsager reciprocity have been criticized because they only model reversible processes in thermodynamic equilibrium [19] (Chap. 7). Furthermore, it is well known that smart materials displaying magnetostriction, piezoelectricity, and thermoelectricity possess a continuum of metastable states whose stability depends on the input variables. The presence of a continuum of metastable states leads to *hysteresis* in the characteristic of the material, which is a non-local memory effect leading to the dependence of the current value of the output on past values of the input. This memory effect is typically modeled using input-state-output formalism, which involves a special class of nonlinear operators characterized by the property of *rate-independence*[1] [20]. The operators describe the relationship between varying stress, strain, electric field, polarization, magnetic field and magnetization by defining the evolution of the memory state associated with the material in an infinite-dimensional metric space. In particular, the operators of Preisach [21] and Prandtl-Ishlinskii [22, 23], which were originally used as models of hysteresis in magnetism and plasticity (as well as for modeling friction, fatigue and sorption [24, 25, 26, 27]), have been successfully adapted for actuation,

[1] An operator $\mathcal{P}$ acting in space of functions of time is called rate-independent if it commutes with any increasing transformation $\tau = \tau(t)$ of the time scale, $\mathcal{P} \circ \tau = \tau \circ \mathcal{P}$.

sensing and energy harvesting applications involving piezoelectric materials [28]. It is important to note that the memory associated with hysteresis in material characteristic is often characterized as "permanent" because there is no explicit time scale set for "forgetting" the effect of past input values.[2] This distinguishes hysteresis from other models of memory such as delay (functional) differential equations or convolution operators. On the other hand, even very small oscillations of the input result in changes of the material state with the associated hysteretic energy losses. This effect is different from bi-stable behavior (often also called "hysteresis") observed, for example, in nonlinear oscillators because bi-stable systems do not manifest hysteresis for small oscillations or, more generally, as long as the system is kept in any one of the two (or more) stable regimes.[3]

The saturation field for Terfenol-D is high, but it shows significant hysteresis in the strain vs field characteristic, suggesting that dissipation of energy due to hysteresis effect can strongly affect energetic performance of an EH device based on this magnetostrictive material. Hysteresis is less significant for Galfenol, but the material saturates at a much lower magnetic field, which is problematic if not accounted for. Therefore, a possible approach to modeling an EH device so that the maximum possible energy is harvested includes the following ingredients: (a) modeling the nonlinearity and hysteresis in the characteristic of a magnetostrictive material that performs energy conversion using a hysteresis operator; (b) modeling electronic and mechanical components of the device with differential equations; (c) combining these two models into a closed operator-differential model of an EH device. The resulting combined model should be amenable to effective analysis that would allow one to maximize the energy output of the device by an appropriate choice of design parameters.

In order to test the above approach in this paper, we focus our attention on improved phenomenological modeling of nonlinear hysteretic characteristics of the magnetostrictive material, while using a simple LR (and LCR) model for the electric circuit. For simplicity, it is assumed that the magnetostrictive material is subject to periodic forcing which is not mediated by a mechanical component. Our aim is to analyze stability of the operator-differential model of the EH device and obtain general properties of the harvested power with respect to a few design parameters that include inductance and resistance of the electric circuit and the magnetic bias.

A few remarks are in order. First, a model for the magnetostrictive material should not only describe the evolution of metastable states for large deformations, but also accurately model the evolution of thermodynamic quantities in non-equilibrium [29] and energy dissipation due to hysteresis. It should therefore be compatible with thermodynamic constraints such as Clausius-Duhem inequality. A thermodynamically consistent, irreversible, nonlinear model for hysteresis and saturation in magnetoelastic materials, involving the Preisach operator, was proposed in [30]. We choose this model because it states the energy balance within the framework of classical thermodynamics in a mathematically rigorous and physically consistent way and reproduces all the basic features of the macroscopic behavior manifested by magnetostrictive materials, including hysteretic response of the magnetization and strain to variations of the applied magnetic field and stress; magnetic response curves affected by the applied pre-stress; magnetic saturation not affected by the applied pre-stress; strain saturation strongly depending on the applied prestress; and, specific scaling of the butterfly-shaped magnetoelastic response curves with the

[2] For example, according to the Preisach model, a permanent magnet does not demagnetize unless a demagnetization field is applied. This is of course an idealization, but a useful one for applications where demagnetization caused by random fluctuations of magnetic moments is slow enough to be negligible on the time interval of interest.

[3] In particular, a control can be applied to avoid, or diminish, the jump phenomenon, i.e. transitions from the desirable stable regime of operation to undesired ones.

applied pre-stress. The model has been fitted to experimental measurements of the constitutive relationship between stress (loading), strain, magnetic field and magnetization in Galfenol and Terfenol-D. Here, we combine this model with a differential equation for the current and voltage in the electric circuit.

Second, hysteresis creates infinitely many degrees of freedom in the state space of the system. As the model of the material characteristic involves the Preisach operator, the phase space of the proposed operator-differential model of the harvester is the space of Lipschitz continuous functions with Lipschitz constant 1, see [31, Chapter II], cf. also [32]. This space lacks a local linear structure. Furthermore, the Preisach operator is not differentiable because, as any other model of hysteretic memory, it is rate-independent. Therefore, some alternative to standard techniques employing linearization is needed in order to analyze stability of solutions to the operator-differential model and address optimization of its parameters. For this reason, we use a method based on variational inequalities combined with a time discretization technique. This discretization technique is also useful for stable numerical implementation of the model.

Third, magnetostrictive materials show a typical butterfly curve with saturation in the strain versus magnetic field characteristic, which means that a biasing magnetic field and correct prestressing need to be applied to extract maximum energy if the harvester is operating in an open-loop fashion[4]. In other words, the magnetic bias determines how much energy is available for harvesting [18]. Therefore, we consider maximization of harvestable energy, for a given mechanical load, with respect to controllable bias field while also taking into account the losses due to lead resistance. In our model, we assume that the stress is periodic. The operating range of frequencies for particular applications is well-known and, in many applications, a relatively narrow frequency band is used for harvesting. For example, the frequency is between 30 to 50 Hz (engine rpm 1800 to 3000) for a harvester in a car engine compartment, and up to 15 Hz for a bridge structure harvester [33, 34].

The paper is organized as follows. In Section 2, we derive a simple differential equation for magnetostrictive harvesting that includes the Preisach hysteresis operator as a model of the magnetostrictive material. Basic properties of the Preisach operator (and its variational form, such as in [35]) are recalled in Section 3. Well-posedness of the initial value problem for the model is established in Section 4. A solution of the harvesting equation is constructed by discretization of time. In Section 5, we show the existence and global asymptotic stability of a periodic solution under periodic forcing. The optimal harvesting problem, formulated as the maximization problem for the energy functional with respect to controllable parameter values, is stated in Section 6. It is proved that an optimal parameter choice exists. Numerical examples are presented in Section 7. For a certain bias current, the delivered power is maximum if the load impedance is the complex conjugate of the output impedance of the harvester, if the harvester is used to continuously power some circuitry. As the magnetostrictive harvester is inductive in nature, one would expect that a capacitive load would maximize the power delivered. We give a numerical evidence that this is indeed the case by comparing circuits with a simple resistive load and a capacitive load.

[4]For Galfenol and Terfenol-D, a bias is typically applied using a permanent magnet; for Metglas, it is applied during manufacture using a transverse magnetic field.

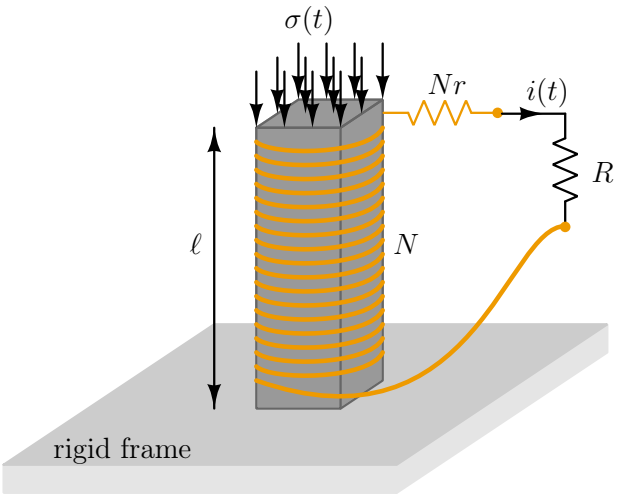

Figure 2: Harvesting device connected to a useful electric load R. The Galfenol core of the coil has section S and length ℓ. The core is subject to periodic uniform stress $\sigma(t)$. The coil has N loops with the total resistance Nr.

2 Harvester model

We consider a simple model consisting of a coil with N loops winding around a Galfenol specimen. An external source forces vibrations of the specimen which, due to coupling between the mechanical and magnetic properties of Galfenol, produce variations of the magnetic field. According to Faraday's law, the resulting electromotive force produces an electric current i in the coil. The coil is connected to a load with resistance R. This resistor models an electric load. We assume that the *active* useful power harvested from the load equals Ri^2. The objective of optimization is to maximize the average harvested power. We also assume that the wire of which the coil is made has finite resistivity ρ that accounts for linear losses in the device. Part of the setting is a permanent magnet which creates a constant field (bias) $B_0 = \mu_0 H_0$ in the coil, where μ_0 is the vacuum permeability.

The total magnetic flux in the coil is $\Phi = NSb$, where b is the magnetic induction, N is the number of loops, and S is the area of a loop which is equal to the area of the cross section of the Galfenol specimen, see Figure 2. By Faraday's law, we have

$$NS\dot{b} = -(R + Nr)i,$$

where r is the resistance of one loop of the coil. The H-field of the current i equals $H_i = Ni/\ell$, where ℓ is the length of the specimen, hence

$$NS\dot{b} = -\frac{(R + Nr)\ell}{N}(h - H_0),$$

where $h = H_i + H_0$ is the total H-field in the specimen. According to the model proposed in [30], the H-field, magnetization m, and stress σ of Galfenol obey the constitutive relationship

$$m = \mathcal{P}\left[\frac{h}{f(\sigma)}, \lambda_{-1}\right], \tag{1}$$

where $\mathcal{P}$ is a Preisach hysteresis operator [36, 37] (see the definition in the next section), λ_{-1} is a given initial memory state, and f is an experimentally determined constitutive function. As $b = \mu_0 h + m$, with this expression for magnetization the Faraday's law becomes

$$\frac{\mathrm{d}}{\mathrm{d}t}\left(\mu_0 h + \mathcal{P}\left[\frac{h}{f(\sigma)}, \lambda_{-1}\right]\right) = \frac{\ell(Nr+R)}{SN^2}\cdot(H_0 - h), \tag{2}$$

where $h = h(t)$ is the unknown function and $\sigma = \sigma(t)$ is the forcing term.

The control parameters in equation (2) are N, ℓ, S, R, and H_0. Assuming periodic forcing $\sigma = \sigma(t)$, we will consider the optimization problem that consists in maximizing the time average value of the useful power

$$W = Ri^2 = R\frac{\ell^2(h-H_0)^2}{N^2}$$

over one period of a periodic process, that is,

$$E = \frac{R\ell^2}{N^2}\int_0^T (h(t) - H_0)^2 \,\mathrm{d}t \to \max \tag{3}$$

where T is the period of the forced periodic solution $h = h(t)$ of equation (2).

3 Preisach operator

Here we recall a definition of the Preisach operator together with a few of its properties which will be used later for analysis of equation (2).

We are given a nonnegative function $\psi \in L^1(\mathbb{R}^2_+)$ (the *Preisach density*), where $\mathbb{R}^2_+ = \{(r,v) : r > 0, v \in \mathbb{R}\}$ is the *Preisach half-plane*. Assume that there exists a function $\psi_1 \in L^1(\mathbb{R})$ such that

$$0 \le \psi(r,v) \le \psi_1(r) \text{ a.e.}, \tag{4}$$

and set

$$\Psi_+ = \int_0^\infty\int_0^\infty \psi(r,v)\,\mathrm{d}v\,\mathrm{d}r\,,\ \Psi_- = \int_0^\infty\int_{-\infty}^0 \psi(r,v)\,\mathrm{d}v\,\mathrm{d}r\,,\ \Psi_1 = \int_0^\infty \psi_1(r)\,\mathrm{d}r\,. \tag{5}$$

The *Preisach state space* is the set

$$\Lambda = \{\lambda \in W^{1,\infty}(0,\infty) : |\lambda'(r)| \le 1 \text{ a.e.}, \lim_{r\to\infty}\lambda(r) = 0\}.$$

For an input function $u = u(t) \in W^{1,1}(0,T)$, an initial state $\lambda_{-1} \in \Lambda$, and a parameter $r > 0$, we define the *play operator* as the solution operator $\mathfrak{p}_r : W^{1,1}(0,T)\times\Lambda \to W^{1,1}(0,T) : (u,\lambda_{-1}) \mapsto \xi_r$ of the variational inequality

$$\begin{aligned} |u(t) - \xi_r(t)| &\le r \quad \forall t \in [0,T]\,, && (6)\\ \xi_r(0) &= \lambda_{-1}(r) + P_r(u(0) - \lambda_{-1}(r))\,, && (7)\\ \dot\xi_r(t)(u(t) - \xi_r(t) - z) &\ge 0 \quad \text{a.e. } \forall z \in [-r,r]\,, && (8)\end{aligned}$$

where P_r is the piecewise linear function

$$P_r(s) = \min\{s + r, \max\{0, s - r\}\}. \tag{9}$$

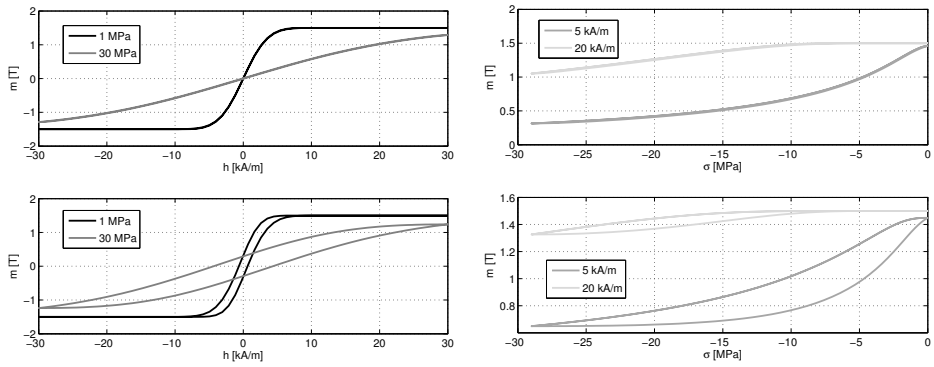

(a) (b)

Figure 3: Hysteresis curves produced by the Preisach model (1) of magnetostrictive material. The density function $\psi(r, v)$ and the function $f(\sigma)$ are defined in Section 7. Behavior with respect to magnetic field h at two different stress values $\sigma_1 = 1$ MPa and $\sigma_2 = 30$ MPa (a) and with respect to compressive stress σ at two different field values $h_1 = 5$ kA/m and $h_2 = 20$ kA/m (b). The upper panels have been obtained for the parameter set presented in Section 7; wider hysteresis loops in the lower panels correspond to a larger parameter $x_0 = 0.4$ with other parameters as in Section 7.

With this choice, the function $\lambda^{(t)}$, which for a fixed time t associates with $r > 0$ the value of the play $\mathfrak{p}_r[u, \lambda_{-1}](t)$, belongs to Λ for each t. Furthermore, the *semigroup property*

$$\mathfrak{p}_r[u, \lambda_{-1}](t + \tau) = \mathfrak{p}_r[u(\cdot + \tau), \mathfrak{p}_r[u, \lambda_{-1}](\tau)](t) \tag{10}$$

holds for each constant time shift $\tau > 0$, see e.g. [36, Section 2.3].

We now introduce the function

$$g(r, v) = \int_0^v \psi(r, s)\,\mathrm{d}s \tag{11}$$

and define the Preisach operator $\mathcal{P}$ by the formula

$$\mathcal{P}[u, \lambda_{-1}](t) = \int_0^\infty g(r, \mathfrak{p}_r[u, \lambda_{-1}](t))\,\mathrm{d}r\,. \tag{12}$$

Figure 3 presents some hysteresis loops produced by relationship (12) between the input $u = h/f(\sigma)$ and the output $m = \mathcal{P}[u, \lambda_{-1}](t)$ of the Preisach operator that mimics the response of magnetization m of a magnetostrictive material to variations of stress σ and magnetic field h.

Furthermore, we introduce the function

$$G(r, v) = \int_0^v s\psi(r, s)\,\mathrm{d}s, \tag{13}$$

and define the *Preisach energy potential*

$$\mathcal{U}[u, \lambda_{-1}](t) = \int_0^\infty G(r, \mathfrak{p}_r[u, \lambda_{-1}](t))\,\mathrm{d}r\,. \tag{14}$$

Then the energy balance equation has the form

$$u(t)\frac{\mathrm{d}}{\mathrm{d}t}\mathcal{P}[u, \lambda_{-1}](t) - \frac{\mathrm{d}}{\mathrm{d}t}\mathcal{U}[u, \lambda_{-1}](t) = \left|\frac{\mathrm{d}}{\mathrm{d}t}\mathcal{D}[u, \lambda_{-1}](t)\right|\,, \tag{15}$$

where

$$\mathcal{D}[u,\lambda_{-1}](t)=\int_0^\infty rg(r,\mathfrak{p}_r[u,\lambda_{-1}](t))\,\mathrm{d}r$$

is the *Preisach dissipation operator*. Relation (15) is a form of the Clausius-Duhem inequality describing dissipation of energy by hysteresis [36, 31, 38].

This definition is shown in [35] to be equivalent to the classical one in [21] based on nonideal relays switching between $+1$ and -1 with thresholds $v-r$ and $v+r$. For each fixed time $t\in[0,T]$, the curve $r\mapsto v=\mathfrak{p}_r[u,\lambda_{-1}](t)$ describes the interface between the $+1$ and -1 regions in the Preisach half-plane $\mathbb{R}^2_+$.

In order to solve Eq. (2) numerically, it is convenient to proceed as in [39] and extend the play operator to the space $G_R(0,T)$ of right continuous regulated functions, that is, functions that are right continuous and admit the left limit at each point of the domain of definition (also called *càdlàg* in the literature). It suffices to replace the variational inequality in differential form (8) by the *Kurzweil integral variational inequality*

$$\int_0^T(u(t)-\xi_r(t)-z(t))\,\mathrm{d}\xi_r(t)\geq 0 \tag{16}$$

for every function $z\in G(0,T)$, $|z(t)|\leq r$ for all $t\in[0,T]$. Of special interest are the so-called *step functions* of the form

$$u(t)=\sum_{j=1}^m u_{j-1}\chi_{[t_{j-1},t_j)}(t)+u_m\chi_{\{t_m\}}(t)\,, \tag{17}$$

where $u_0,u_1,\dots u_m$ are constants and $\chi_A(t)$ denotes the characteristic function of a set A, that is, $\chi_A(t)=1$ if $t\in A$, $\chi_A(t)=0$ if $t\notin A$. We then have

$$\mathfrak{p}_r[u,\lambda_{-1}](t)=\sum_{j=1}^m \lambda_{j-1}(r)\chi_{[t_{j-1},t_j)}(t)+\lambda_m(r)\chi_{\{t_m\}}(t)\,, \tag{18}$$

where $\lambda_j\in\Lambda$ are defined recurrently by a formula similar to (7)

$$\lambda_j(r)=\lambda_{j-1}(r)+P_r(u_j-\lambda_{j-1}(r))\ \text{ for }\ j=0,1,\dots,m\,, \tag{19}$$

where P_r is the function (9). We have the saturation bound

$$-\Psi_-\leq\mathcal{P}[u,\lambda_{-1}](t)\leq\Psi_+ \tag{20}$$

for all $u\in G_R(0,T)$, $\lambda_{-1}\in\Lambda$, and $t\in[0,T]$, as well as the Lipschitz continuous dependence for two inputs $u_1,u_2\in G_R(0,T)$, $\lambda^1_{-1},\lambda^2_{-1}\in\Lambda$, see [39],

$$|\mathfrak{p}_r[u_1,\lambda^1_{-1}](t)-\mathfrak{p}_r[u_2,\lambda^2_{-1}](t)| \;\leq\; \max\{|u_1-u_2|_{[0,t]}\,,|\lambda^1_{-1}(r)-\lambda^2_{-1}(r)|\}, \tag{21}$$

$$|\mathcal{P}[u_1,\lambda^1_{-1}](t)-\mathcal{P}[u_2,\lambda^2_{-1}](t)| \;\leq\; \Psi_1|u_1-u_2|_{[0,t]}+\int_0^\infty\psi_1(r)|\lambda^1_{-1}(r)-\lambda^2_{-1}(r)|\,\mathrm{d}r, \tag{22}$$

where for a function $w:[0,T]\to\mathbb{R}$ and $0\leq s<t\leq T$ we set $|w|_{[s,t]}=\sup_{\tau\in[s,t]}|w(\tau)|$.

We recall here the Hilpert inequality, see [40], which we systematically use in the sequel.

Lemma 1 *For $u_1, u_2 \in W^{1,1}(0,T)$ and $\lambda^1_{-1}, \lambda^2_{-1} \in \Lambda$ put $\xi^i_r(t) = \mathfrak{p}_r[u_i, \lambda^i_{-1}](t)$, $i = 1, 2$. Then for every locally Lipschitz continuous non-decreasing function $g : \mathbb{R} \to \mathbb{R}$ and a.e. $t \in (0,T)$ we have*

$$\frac{\mathrm{d}}{\mathrm{d}t} \left| g(\xi^1_r) - g(\xi^2_r) \right| (t) \;\le\; \operatorname{sign}\left(u_1(t) - u_2(t)\right) \frac{\mathrm{d}}{\mathrm{d}t} \left(g(\xi^1_r) - g(\xi^2_r) \right) (t)\,. \tag{23}$$

Proof. From (6)–(8) it follows that (we omit the argument t for simplicity)

$$\begin{aligned} g'(\xi^1_r)\, \dot{\xi}^1_r \left((u_1 - \xi^1_r) - (u_2 - \xi^2_r) \right) &\;\ge\; 0 \quad \text{a.e.,} \\ -g'(\xi^2_r)\, \dot{\xi}^2_r \left((u_1 - \xi^1_r) - (u_2 - \xi^2_r) \right) &\;\ge\; 0 \quad \text{a.e.,} \end{aligned}$$

hence

$$\left((u_1 - \xi^1_r) - (u_2 - \xi^2_r) \right) \frac{\mathrm{d}}{\mathrm{d}t} \left(g(\xi^1_r) - g(\xi^2_r) \right) \ge 0 \quad \text{a.e.} \tag{24}$$

Using the implication $c(a-b) \ge 0 \;\Rightarrow\; c(\operatorname{sign} a - \operatorname{sign} b) \ge 0$ for $a, b, c \in \mathbb{R}$, we obtain from (24) that

$$\operatorname{sign}\left(\xi^1_r - \xi^2_r\right) \frac{\mathrm{d}}{\mathrm{d}t} \left(g(\xi^1_r) - g(\xi^2_r) \right) \;\le\; \operatorname{sign}\left(u_1 - u_2\right) \frac{\mathrm{d}}{\mathrm{d}t} \left(g(\xi^1_r) - g(\xi^2_r) \right) \quad \text{a.e.} \tag{25}$$

For a.e. $t > 0$ we have

$$\begin{aligned} g(\xi^1_r(t)) = g(\xi^2_r(t)) \quad &\Rightarrow \quad \frac{\mathrm{d}}{\mathrm{d}t} \left| g(\xi^1_r) - g(\xi^2_r) \right| (t) = 0\,, \\ g(\xi^1_r(t)) \ne g(\xi^2_r(t)) \quad &\Rightarrow \quad \operatorname{sign}\left(\xi^1_r(t)\right) - \xi^2_r(t)) = \operatorname{sign}\left(g(\xi^1_r(t)) - g(\xi^2_r(t))\right), \end{aligned}$$

and (23) follows. ∎

4 Qualitative properties of solutions

In this section, we prove well-posedness of model equation (2). This equation is different from the operator-differential equations with the Preisach operator considered in [35, 41, 27, 42, 26, 43] as the input of the Preisach operator contains the forcing term. That is, we consider a Preisach operator $\mathcal{P}$ as in Section 3, with initial memory λ_{-1}. The harvesting process is modeled by Eq. (2) with a given external forcing $f(t) := f(\sigma(t)) > 0$, given bias magnetic field h_0, and given material constants. Although the case of constant bias field is of main interest to us, in this and the next sections we allow $h_0 = h_0(t)$ to depend on time.

We thus consider the differential equation for the unknown magnetic field $h(t)$

$$\frac{\mathrm{d}}{\mathrm{d}t} \left(\mu_0 h(t) + \mathcal{P}\left[\frac{h}{f}, \lambda_{-1} \right] (t) \right) + \alpha(h(t) - h_0(t)) = 0 \tag{26}$$

with given $h_0(t)$, where the magnetic induction $b(t)$ is given by

$$b(t) = \mu_0 h(t) + \mathcal{P}\left[\frac{h}{f}, \lambda_{-1} \right] (t)\,, \tag{27}$$

and

$$\alpha = \frac{\ell(Nr+R)}{SN^2}.$$

Introducing a new unknown function $u(t) = h(t)/f(t)$, we rewrite (26) in the form

$$\frac{\mathrm{d}}{\mathrm{d}t}\big(\mu_0 f(t)u(t) + \mathcal{P}[u,\lambda_{-1}](t)\big) + \alpha(f(t)u(t) - h_0(t)) = 0\,. \tag{28}$$

Proposition 2 *Let $h_0 \in L^\infty(0,T)$, $f \in W^{1,2}(0,T)$, $\lambda_{-1} \in \Lambda$, and an initial condition $u_0 \in \mathbb{R}$ be given, $0 < f_* \le f(t) \le f^*$ for all $t \in [0,T]$, $\int_0^T |\dot f(t)|^2\,\mathrm{d}t \le F_0$, $|h_0(t)| \le H_0$ a.e., where f_*, f^*, F_0, H_0 are fixed constants. Then there exists a unique solution $u \in W^{1,2}(0,T)$ of* (28) *such that $u(0) = u_0$, and* (28) *holds a.e. in $(0,T)$. This solution continuously depends on initial data u_0, λ_{-1} and functions f, h_0 in the uniform norm.*

Proof. Set

$$y(t) = \mu_0 u(t) + \frac{1}{f(t)}\mathcal{P}[u,\lambda_{-1}](t). \tag{29}$$

By [44, Theorem 3.4], for every given function y in the space $C[0,T]$ of continuous functions on $[0,T]$ there exists a unique $u \in C[0,T]$ such that (29) holds for all t. Moreover, the mapping $u = \mathcal{G}[y,f]$ which with y and f associates u is causal and Lipschitz continuous in $C[0,T]\times C[0,T]$. Hence, Eq. (28) can be interpreted as integral equation for the unknown function y

$$f(t)y(t) = f(0)y(0) + \alpha\int_0^t (h_0(\tau) - f(\tau)\mathcal{G}[y,f](\tau))\,\mathrm{d}\tau, \tag{30}$$

the unique solution of which can be easily constructed by successive approximations.

In order to prove that the solution of (28) depends continuously on the data, we now choose two sets of data $(\lambda^1_{-1}, u^1_0, f_1, h^1_0)$, $(\lambda^2_{-1}, u^2_0, f_2, h^2_0)$ satisfying the assumptions of Proposition 2, and denote by u_1, u_2 the corresponding solutions of (28). As in the uniqueness proof, we multiply the difference of the two equations (28) written for u_1 and u_2 by $\operatorname{sign}(u_1(t)-u_2(t))$, and use the fact that $\operatorname{sign}(u_1(t)-u_2(t)) = \operatorname{sign}(f_1(t)(u_1(t)-u_2(t)))$. The Hilpert inequality (23) now yields (we omit the arguments (t) for simplicity)

$$\begin{aligned}\frac{\mathrm{d}}{\mathrm{d}t}\Big(\mu_0 f_1|u_1-u_2| + \int_0^\infty |g(r,\mathfrak{p}_r[u_1,\lambda^1_{-1}]) - g(r,\mathfrak{p}_r[u_2,\lambda^2_{-1}])|\,\mathrm{d}r\Big) + \alpha f_1|u_1-u_2| \\ \le\ \mu_0|\dot u_2||f_1-f_2| + \mu_0|u_2||\dot f_1-\dot f_2| + \alpha|u_2||f_1-f_2| + \alpha|h^1_0-h^2_0|.\end{aligned} \tag{31}$$

Integrating from 0 to t we conclude that there exists a constant C_1 depending only on the bounds for the data such that

$$\begin{aligned}|u_1-u_2|_{[0,T]} \ \le\ C_1\Big(&|u^1_0-u^2_0| + \int_0^\infty \psi_1(r)|\lambda^1_{-1}-\lambda^2_{-1}|(r)\,\mathrm{d}r \\ &+ \int_0^T |\dot f_1-\dot f_2|\,\mathrm{d}t + \Big(\int_0^T |f_1-f_2|^2\,\mathrm{d}t\Big)^{1/2} + \int_0^T |h^1_0-h^2_0|\,\mathrm{d}t.\end{aligned} \tag{32}$$

■

5 Global stability of the periodic regime

Next, we consider time periodic data, that is, there exists $T > 0$ such that the identities

$$h_0(t+T) = h_0(t)\,, \quad f(t+T) = f(t) \tag{33}$$

hold for all $t \geq 0$. We prove the following result.

Proposition 3 *Let f, h_0 be defined on $[0,\infty)$ and satisfy* (33)*, and let the hypotheses of Proposition 2 hold. Then there exists a unique function u_* with the following properties:*

(i) $u_*(t+T) = u_*(t) \quad \forall t \geq 0\,, \quad u_*\big|_{[0,T]} \in W^{1,2}(0,T)\,;$

(ii) *Let u be the solution of* (28) *on $[0,\infty)$ with initial data $u_0 \in \mathbb{R}$, $\lambda_{-1} \in \Lambda$. Then there exists $\lambda_* \in \Lambda$ such that*

$$\frac{\mathrm{d}}{\mathrm{d}t}\big(\mu_0 f(t)u_*(t) + \mathcal{P}[u_*,\lambda_*](t)\big) + \alpha(f(t)u_*(t) - h_0(t)) = 0 \ \textit{a.e.}, \tag{34}$$

$$\lim_{t\to\infty} |u(t) - u_*(t)| = 0. \tag{35}$$

The meaning of Proposition 3 is that Eq. (28) with periodic data has a unique periodic solution which is globally asymptotically stable. On the other hand, the limit memory state λ_* is not uniquely determined, but the values of $\mathcal{P}[u_*,\lambda_*](t)$ for different λ_* differ only by an additive constant.

Proof of Proposition 3. Let u be as in (ii). We test Eq. (28) by $\operatorname{sign}(u(t)) = \operatorname{sign}(f(t)u(t))$ and refer to Lemma 1 with $u_1 = u$, $u_2 = 0$ to obtain

$$\frac{\mathrm{d}}{\mathrm{d}t}\left(\mu_0 f(t)|u(t)| + \int_0^\infty |g(r,\mathfrak{p}_r[u,\lambda_{-1}](t))|\,\mathrm{d}r\right) + \alpha f(t)|u(t)| \leq \alpha|h_0(t)|\,, \tag{36}$$

and we easily conclude that there exists a constant C_2 such that $|u(t)| \leq C_2$ for all $t \geq 0$. Furthermore, multiplying (28) by $\dot u(t)$ and using the fact that $\dot{\mathcal{P}}[u,\lambda_{-1}]\dot u \geq 0$ a.e., we obtain

$$\mu_0(f(t)\dot u^2(t) + u(t)\dot f(t)\dot u(t)) + \alpha f(t)u(t)\dot u(t) \leq \alpha h_0(t)\dot u(t),$$

hence there exists a constant $C_3 > 0$ such that

$$\int_\tau^{\tau+T} \dot u^2(t)\,\mathrm{d}t \leq C_3 \tag{37}$$

independently of $\tau \geq 0$.

We now subtract the two equations (28) taken at t and $t+T$, and obtain

$$\frac{\mathrm{d}}{\mathrm{d}t}\big(\mu_0 f(t)(u(t+T)-u(t)) + (\mathcal{P}[u,\lambda_{-1}](t+T) - \mathcal{P}[u,\lambda_{-1}](t))\big) + \alpha f(t)(u(t+T)-u(t)) = 0\,. \tag{38}$$

We proceed as above, multiplying (38) by $\operatorname{sign}(u(t+T)-u(t))$. From Hilpert's inequality it follows that

$$\frac{\mathrm{d}}{\mathrm{d}t}\Big(\mu_0 f(t)|u(t+T)-u(t)| + \int_0^\infty |g(r,\mathfrak{p}_r[u,\lambda_{-1}])(t+T) - g(r,\mathfrak{p}_r[u,\lambda_{-1}])(t)|\,\mathrm{d}r\Big) + \alpha f(t)|u(t+T)-u(t)| \ \leq\ 0. \tag{39}$$

For $k \in \mathbb{N}$ put

$$B_k = \mu_0 f(0)|u((k+1)T) - u(kT)| + \int_0^\infty |g(r, \mathfrak{p}_r[u, \lambda_{-1}])((k+1)T) - g(r, \mathfrak{p}_r[u, \lambda_{-1}])(kT)| \, \mathrm{d}r.$$

By virtue of (39), we have for $n > k$ that

$$\alpha \int_{kT}^{nT} f(t)|u(t+T) - u(t)| \, \mathrm{d}t \le B_k - B_n.$$

We now introduce the sequence

$$u_j(t) = u(t + jT)$$

for $j \in \mathbb{N}$ and $t \in [0, T]$. We have

$$\begin{aligned} \alpha \int_0^T f(t)|u_{n+1}(t) - u_k(t)| \, \mathrm{d}t &\le \alpha \sum_{j=k}^{n} \int_0^T f(t)|u_{j+1}(t) - u_j(t)| \, \mathrm{d}t \\ &= \alpha \int_{kT}^{nT} f(t)|u(t+T) - u(t)| \, \mathrm{d}t \le B_k - B_n. \end{aligned} \tag{40}$$

The sequence B_k is decreasing and positive, hence it is convergent. Consequently, u_j is a Cauchy sequence in $L^1(0, T)$. Furthermore, we know that the sequence u_j is bounded in $C[0, T]$ and, by (37), also in $W^{1,2}(0, T)$. We conclude that u_j is convergent uniformly in $C[0, T]$ and weakly in $W^{1,2}(0, T)$. Let $u_* \in W^{1,2}(0, T)$ be its limit. Letting k and n tend to ∞ in (40), we obtain

$$u_*(t + T) = u_*(t)$$

for all $t \ge 0$, hence u_* is periodic. Furthermore, for $t \in [nT, (n + 1)T]$ we have $u(t) - u_*(t) = u_n(t - nT) - u_*(t - nT)$, hence (35) holds.

It remains to prove that u_* is a solution of (34) with a suitable choice of λ^* and that it is unique. For $n \in \mathbb{N}$ put

$$\lambda_n(r) = \mathfrak{p}_r[u, \lambda_{-1}](nT), \tag{41}$$

with the intention to prove that λ_n converge in Λ. Let $k \in \mathbb{N}$ be fixed for the moment, and let us define

$$u^{(k)}(t) = \begin{cases} u(t) & \text{for } t \in [0, kT], \\ u_*(t) - u_*(kT) + u(kT) & \text{for } t > kT. \end{cases} \tag{42}$$

By [37, Section 2.8], the function $\mathfrak{p}_r[u^{(k)}, \lambda_{-1}](t)$ is T-periodic for $t \ge (k + 1)T$. Hence, for $n > k$, we have

$$\mathfrak{p}_r[u^{(k)}, \lambda_{-1}](nT) = \mathfrak{p}_r[u^{(k)}, \lambda_{-1}]((k + 1)T)$$

and consequently, by triangle inequality,

$$\begin{aligned} |\lambda_n(r) - \lambda_{k+1}(r)| \le\ & |\mathfrak{p}_r[u, \lambda_{-1}](nT) - \mathfrak{p}_r[u^{(k)}, \lambda_{-1}](nT)| \\ & + |\mathfrak{p}_r[u, \lambda_{-1}]((k + 1)T) - \mathfrak{p}_r[u^{(k)}, \lambda_{-1}]((k + 1)T)| \end{aligned}$$

for all $r > 0$. Using (21) and (42), we obtain

$$|\lambda_n(r) - \lambda_{k+1}(r)| \le 4|u - u_*|_{[kT, \infty)}.$$

hence $\{\lambda_n(r)\}$ is a Cauchy sequence uniform in r. The set Λ is closed with respect to uniform convergence, hence there exists $\lambda_* \in \Lambda$ such that

$$\lim_{n\to\infty} \sup_{r>0} |\lambda_n(r) - \lambda_*(r)| = 0.$$

From the semigroup property (10) it follows that

$$\mathfrak{p}_r[u_n, \lambda_n](t) = \mathfrak{p}_r[u, \lambda_{-1}](t + nT) \tag{43}$$

for all $n \in \mathbb{N}$ and $t \geq 0$. By (28) we thus have for all n that

$$\frac{\mathrm{d}}{\mathrm{d}t}\big(\mu_0 f(t)u_n(t) + \mathcal{P}[u_n, \lambda_n](t)\big) + \alpha(f(t)u_n(t) - h_0(t)) = 0 \text{ a.e.}, \tag{44}$$

and passing to the limit as $n \to \infty$ we obtain (34). Uniqueness of u_* follows easily again from Hilpert's inequality. ■

6 Harvesting efficiency

Let us consider the case that the external magnetic field (bias) is constant, that is,

$$h_0(t) \equiv H_0 \text{ for } t \geq 0,$$

and $f(t)$ is a given T-periodic function. Let $u(t)$ be the T-periodic solution of the equation

$$\frac{\mathrm{d}}{\mathrm{d}t}\big(\mu_0 f(t)u(t) + \mathcal{P}[u, \lambda](t)\big) + \alpha(f(t)u(t) - H_0) = 0 \tag{45}$$

with a fixed choice of $\lambda \in \Lambda$. In agreement with Eq. (3), the optimal harvesting problem consists in choosing the parameters $H_0 \in \mathbb{R}$, and $\alpha, \gamma > 0$ in order to maximize the harvested energy

$$E(H_0, \alpha, \gamma) = \gamma \int_0^T (H_0 - h(t))^2 \,\mathrm{d}t \tag{46}$$

under given loading $f(t)$, with $h(t) = f(t)u(t)$, where

$$\gamma = \frac{R\ell^2}{N^2}, \qquad \alpha = \frac{\ell(Nr + R)}{SN^2}. \tag{47}$$

Parameters α and γ are controlled by four physical parameter: the number of turns in the coil, N, the electric load (resistance), R, and the dimensions of the Galfenol specimen, ℓ and S. Note that γ/α is bounded above by the constant ℓS, which is the volume of the specimen. The magnetic bias H_0 is an independent parameter.

Using (45), we alternatively have

$$E(H_0, \alpha, \gamma) = \frac{\gamma}{\alpha^2} \int_0^T \dot{b}(t)^2 \,\mathrm{d}t \tag{48}$$

with b as in (27). In view of (5), we define auxiliary functions

$$\begin{array}{rcll} k_+(U) & = & \int_0^U \int_0^{U-r} \psi(r, v) \,\mathrm{d}v \,\mathrm{d}r - \int_U^\infty \int_{U-r}^0 \psi(r, v) \,\mathrm{d}v \,\mathrm{d}r & \text{for } U > 0\,, \\ k_-(U) & = & -\int_0^{-U} \int_{U+r}^0 \psi(r, v) \,\mathrm{d}v \,\mathrm{d}r + \int_{-U}^\infty \int_0^{U+r} \psi(r, v) \,\mathrm{d}v \,\mathrm{d}r & \text{for } U < 0\,, \end{array} \tag{49}$$

and by hypothesis we have $\lim_{U\to\infty} k_+(U) = \Psi_+$, $\lim_{U\to-\infty} k_-(U) = -\Psi_-$. We now prove the following statement.

Proposition 4 *Assume that there exist* $k_0 > 0$ *and* $\delta > 0$ *such that the functions* $k_\pm$ *in* (49) *have the property*

$$k_+(U) \geq \Psi_+ - k_0 U^{-1-\delta} \text{ for } U > 0\,,\ k_-(U) \leq -\Psi_- + k_0|U|^{-1-\delta} \text{ for } U < 0\,. \quad (50)$$

Then there exist constants $C_1^*, C_2^*, C_3^*, C_4^*$ *independent of* H_0 *and* α *such that*

$$E(H_0,\alpha,\gamma) \leq \begin{cases} C_1^*\gamma\,, \\ C_2^*\gamma|H_0|\,, \\ C_3^*\gamma\alpha^{-2}(1+|H_0|)^2\,, \\ C_4^*\gamma(1+|H_0|)^{-2-2\delta}\,. \end{cases} \quad (51)$$

Corollary 5 *We have the uniform limits*

$$\begin{array}{ll} \lim_{\gamma\to 0} E(H_0,\alpha,\gamma) = 0\,, & \lim_{\alpha\to\infty} E(H_0,\alpha,\gamma) = 0\,, \\ \lim_{|H_0|\to 0} E(H_0,\alpha,\gamma) = 0\,, & \lim_{|H_0|\to\infty} E(H_0,\alpha,\gamma) = 0\,. \end{array} \quad (52)$$

In particular, there exist positive constants A_+, A_-, H_+, H_- *such that* $E(H_0,\alpha,\gamma)$ *admits a global maximal value which is reached in the domain* $\Omega_0 := \{(H_0,\alpha,\gamma) \in \mathbb{R}^3 : A_- < \gamma \leq \alpha\ell S < A_+\,,\ H_- < |H_0| < H_+\}$.

We first show how Corollary 5 follows from Proposition 4.

Proof of Corollary 5. For two different parameter values $(H_0^1,\alpha_1), (H_0^2,\alpha_2)$, let u_1, u_2 be the corresponding periodic solutions of (45) and λ_1, λ_2 the corresponding memory states. We test the difference of Eqs. (45) written for u_1 and u_2 by $\operatorname{sign}(u_1-u_2)$ and use the fact that $\operatorname{sign}(u_1-u_2) = \operatorname{sign}(fu_1 - fu_2)$ to obtain

$$\int_0^T \big(\alpha_1(f(t)u_1(t) - H_0^1) - \alpha_2(f(t)u_2(t) - H_0^2)\big)\operatorname{sign}(u_1-u_2)\,\mathrm{d}t \leq 0,$$

hence

$$\int_0^T \alpha_1 f(t)|u_1(t)-u_2(t)|\,\mathrm{d}t \leq \int_0^T |\alpha_1-\alpha_2|f(t)|u_2(t)|\,\mathrm{d}t + T|\alpha_1 H_0^1 - \alpha_2 H_0^2|\,.$$

It follows that the solution u depends locally Lipschitz continuously on α and H_0, and we conclude that $E(H_0,\alpha,\gamma)$ is locally Lipschitz in all variables.

As a consequence of Proposition 4 and of the inequality $\gamma/\alpha \leq \ell S$, we have the inequalities

$$\begin{cases} E(H_0,\alpha,\gamma) & \leq C_1^*\gamma\,, \\ E(H_0,\alpha,\gamma)^{2+\delta} & \leq C_4^*(C_3^*)^{1+\delta}(\ell S)^{2+\delta}\alpha^{-\delta}\,, \\ E(H_0,\alpha,\gamma)^2 & \leq C_2^*C_3^*(\ell S)^2|H_0|(1+|H_0|)^2\,, \\ E(H_0,\alpha,\gamma)^2 & \leq C_3^*C_4^*(\ell S)^2(1+|H_0|)^{-2\delta}\,, \end{cases} \quad (53)$$

which imply the uniform limits. These limits, the estimate $E > 0$ and the Lipschitz continuity of $E = E(H_0,\alpha,\gamma)$ imply that E admits a maximum. ■

Proof of Proposition 4. We first derive some *a priori* bounds for the periodic solutions of (45). To this end, we rewrite (45) in the form

$$\frac{\mathrm{d}}{\mathrm{d}t}\big(\mu_0(h(t)-H_0)+\mathcal{P}[u,\lambda](t)\big) + \frac{\alpha}{\mu_0}\big(\mu_0(h(t)-H_0)+\mathcal{P}[u,\lambda](t)\big) = \frac{\alpha}{\mu_0}\mathcal{P}[u,\lambda](t). \quad (54)$$

This is an equation of the form

$$\frac{\mu_0}{\alpha}\dot{B}(t) + B(t) = p(t), \tag{55}$$

with $B(t) = \mu_0(h(t) - H_0) + \mathcal{P}[u,\lambda](t)$, and $p(t) = \mathcal{P}[u,\lambda](t)$, which is bounded in absolute value by the saturation value $\Psi_0 := \max\{\Psi_+, \Psi_-\}$. We multiply (55) by $B(t)|B(t)|^{q-2}$ for sufficiently large exponents q and integrate from 0 to T. We obtain

$$\int_0^T |B(t)|^q \,\mathrm{d}t \le \int_0^T |p(t)||B(t)|^{q-1} \,\mathrm{d}t \le \Big(\int_0^T |p(t)|^q \,\mathrm{d}t\Big)^{1/q} \Big(\int_0^T |B(t)|^q \,\mathrm{d}t\Big)^{(q-1)/q},$$

hence

$$\Big(\int_0^T |B(t)|^q \,\mathrm{d}t\Big)^{1/q} \le \Big(\int_0^T |p(t)|^q \,\mathrm{d}t\Big)^{1/q} \le \Psi_0 T^{1/q}.$$

Letting q tend to ∞, we conclude that

$$|B(t)| \le \Psi_0 \quad \forall t \in [0,T]. \tag{56}$$

This implies that

$$|h(t) - H_0| \le \frac{2}{\mu_0}\Psi_0 \quad \forall t \in [0,T]. \tag{57}$$

This and (46) immediately yield the first inequality in (51) with $C_1^* = (4T/\mu_0^2)\Psi_0^2$. Furthermore, multiplying (45) by $\operatorname{sign} u(t) = \operatorname{sign} h(t)$, we obtain by Hilpert's inequality (Lemma 1) with $u_2 = 0$, $\lambda_{-1}^2 = 0$ that $\int_0^T |h(t)| \,\mathrm{d}t \le T|H_0|$, and using again (57), we obtain the second inequality in (51) with $C_2^* = (4T/\mu_0)\Psi_0$.

We now investigate the cases that $|H_0|$ or α are large. We test (45) by $\dot{h}(t)$ and obtain

$$\int_0^T \Big(\mu_0|\dot{h}(t)|^2 + \dot{\mathcal{P}}[u,\lambda](t)(f(t)\dot{u}(t) + \dot{f}(t)u(t))\Big) \,\mathrm{d}t = 0.$$

We have

$$0 \le \dot{\mathcal{P}}[u,\lambda](t)\dot{u}(t) \le \Psi_1|\dot{u}(t)|^2\,, \tag{58}$$

hence

$$\mu_0 \int_0^T |\dot{h}(t)|^2 \,\mathrm{d}t \le \int_0^T |\dot{\mathcal{P}}[u,\lambda](t)\dot{f}(t)u(t)| \,\mathrm{d}t \le \int_0^T \Psi_1|\dot{u}(t)|\,|\dot{f}(t)|\,|u(t)| \,\mathrm{d}t\,.$$

We now substitute $u = h/f$, and obtain, using also Young's inequality,

$$\begin{aligned}
\mu_0 \int_0^T |\dot{h}(t)|^2 \,\mathrm{d}t &\le \int_0^T \Psi_1|h(t)|\frac{|\dot{f}(t)|}{f(t)}\left(\frac{|\dot{h}(t)|}{f(t)} + \frac{|h(t)\dot{f}(t)|}{f^2(t)}\right) \mathrm{d}t \\
&\le \frac{\mu_0}{2}\int_0^T |\dot{h}(t)|^2 \,\mathrm{d}t + C_\mu \int_0^T |h(t)|^2|\dot{f}(t)|^2 \,\mathrm{d}t,
\end{aligned} \tag{59}$$

with a suitably chosen constant C_μ. From (57) and the hypotheses on $\dot{f}$ we thus find a constant C_4 such that

$$\int_0^T |\dot{h}(t)|^2 \,\mathrm{d}t \le C_4(1 + |H_0|)^2.$$

We have as before by (57) that

$$\int_0^T |\dot{u}(t)|^2 \,\mathrm{d}t \le C_5 \left(\int_0^T |\dot{h}(t)|^2 \,\mathrm{d}t + (1+|H_0|)^2 \right),$$

hence, by (58),

$$\int_0^T |\dot{b}(t)|^2 \,\mathrm{d}t \le C_6 (1+|H_0|)^2$$

with suitably chosen constants C_5, C_6, and we conclude from (48) that the third inequality in (51) holds with $C_3^* = C_6$.

The last inequality is more involved. We first notice that by (57), we have $h(t) \ge H_0 - (2/\mu_0)\Psi_0$ for all $t \in [0,T]$. For any $U > 0$ put $H_0 := f^* U + (2/\mu_0)\Psi_0$. Then

$$u(t) = \frac{h(t)}{f(t)} \ge \frac{f^*}{f(t)} U \ge U \;\forall t \in [0,T].$$

Consequently, $\mathfrak{p}_r[u,\lambda](t) \ge U - r$ for all t, and

$$\Psi_+ \ge \mathcal{P}[u,\lambda](t) \ge \int_0^\infty g(r, U-r)\,\mathrm{d}r = k_+(U) \;\forall t \in [0,T].$$

We now rewrite (54) as

$$\frac{\mathrm{d}}{\mathrm{d}t}\big(\mu_0(h(t)-H_0)+\mathcal{P}[u,\lambda](t)-\Psi_+\big)+\frac{\alpha}{\mu_0}\big(\mu_0(h(t)-H_0)+\mathcal{P}[u,\lambda](t)-\Psi_+\big) = \frac{\alpha}{\mu_0}(\mathcal{P}[u,\lambda](t)-\Psi_+). \tag{60}$$

This is again an equation of the form (55) with $B(t) = \mu_0(h(t)-H_0)+\mathcal{P}[u,\lambda](t)-\Psi_+$, and $p(t) = \mathcal{P}[u,\lambda](t) - \Psi_+$ We argue as above, and the counterpart of (56) reads, by hypothesis on $k_+(U)$,

$$|\mu_0(h(t)-H_0)+\mathcal{P}[u,\lambda](t)-\Psi_+| \le \max_t |\mathcal{P}[u,\lambda](t)-\Psi_+| \le \Psi_+ - k_+(U) \le k_0 U^{-1-\delta},$$

hence

$$|h(t)-H_0| \le \frac{2k_0}{\mu_0} U^{-1-\delta} = \frac{2k_0}{\mu_0}\left(\frac{1}{f^*}\left(H_0 - \frac{2}{\mu_0}\Psi_0\right)\right)^{-1-\delta}.$$

The argument is similar for H_0 large negative. Thus, the fourth inequality in (51) follows if $|H_0| > (4/\mu_0)\Psi_0$. For $|H_0| \le (4/\mu_0)\Psi_0$, it suffices to take C_4^* larger than a suitable multiple of C_1^*. Proposition 4 is proved. ■

Corollary 5 guarantees the existence of solution to the optimization problem (3) which aims at maximization of the output power of the harvester. To estimate the efficiency of the harvester and the relative amount of energy losses, one can use the energy balance law from [30]

$$\dot{\varepsilon}\sigma + \dot{b}h - \frac{\mathrm{d}}{\mathrm{d}t}\mathcal{V}[\sigma,h] = D[\sigma,h], \tag{61}$$

where $\mathcal{V}$ is the magnetostrictive potential of the form (we omit the initial state λ_{-1} for simplicity)

$$\mathcal{V}[\sigma,h] = (f(\sigma) - \sigma f'(\sigma))\mathcal{U}[h/f(\sigma)], \tag{62}$$

with $\mathcal{U}$ as in (14); the hysteresis dissipation $D[\sigma,h]$ is given by the formula

$$D[\sigma,h] = f(\sigma)\left|\frac{\mathrm{d}}{\mathrm{d}t}\mathcal{D}[h/f(\sigma)]\right| \tag{63}$$

with the Preisach dissipation operator $\mathcal{D}$ as in (15); and, the magnetostriction ε can be computed from the relationship [30]

$$\varepsilon = -f'(\sigma)\mathcal{U}[h/f(\sigma)]. \tag{64}$$

Let us consider the T-periodic process described by Eq. (45). In view of the derivation in Section 2 and Eq. (45), the harvested energy over one period is given by

$$E(H_0, \alpha, \gamma) = -\frac{\gamma}{\alpha}\int_0^T \dot{b}(t)h(t)\,\mathrm{d}t. \tag{65}$$

The mechanical energy per unit volume supplied to the system over one period is, by virtue of (61) (note that the process is periodic),

$$\int_0^T \dot{\varepsilon}(t)\sigma(t)\,\mathrm{d}t = \frac{\alpha}{\gamma}E(H_0, \alpha, \gamma) + \int_0^T D[\sigma, h]\,\mathrm{d}t. \tag{66}$$

The volume of the specimen is $S\ell$. Hence, if we define the efficiency Δ as the ratio between the harvested energy and the supplied energy, we obtain

$$\Delta = \frac{\frac{1}{S\ell}E(H_0, \alpha, \gamma)}{\frac{\alpha}{\gamma}E(H_0, \alpha, \gamma) + \int_0^T D[\sigma, h]\,\mathrm{d}t} = \frac{-\frac{R}{Nr+R}\int_0^T \dot{b}(t)h(t)\,\mathrm{d}t}{-\int_0^T \dot{b}(t)h(t)\,\mathrm{d}t + \int_0^T D[\sigma, h]\,\mathrm{d}t}. \tag{67}$$

Note that the efficiency is a number between 0 and 1. The integral $\int_0^T \dot{b}(t)h(t)\,\mathrm{d}t$ is negative by virtue of (65). Geometrically, this corresponds to the fact that the trajectory of the periodic solution in the $h - b$ plane forms a closed clockwise loop. If no hysteresis dissipation D is present, the efficiency is equal to the ratio between the resistance of the electric load and the total resistance of the contour including the coil resistance.

7 Numerical examples

Assuming that the specimen and the wire have circular cross section and the radius of the cross section of the wire is d, the length of one loop of wire equals $2\sqrt{\pi S}$ and its resistance is

$$r = \frac{2\sqrt{\pi S}\rho}{\pi d^2}.$$

We fix an exemplary set of physical parameters

$$\ell = 18\,mm,\ S = 9\,mm^2,\ d = 0.1\,mm,\ \rho = 1.68 \times 10^{-8}\,\Omega \cdot m,\ N = 2000$$

with ρ being the resistivity of copper; the vacuum permiability is $\mu_0 = 4\pi \times 10^{-7}\frac{H}{m}$. The density function ψ of the Preisach operator $\mathcal{P}$ and the function $f = f(\sigma)$ were fit to experimental measurements on Galfenol in [30]. We simulate equation (2) using these fitted functions that are defined by the relations

$$f(\sigma) = c\left(c_f + c_e\pi\sigma + \frac{c_a}{c_b}\,\mathrm{e}^{c_b\pi\sigma} + \frac{c_c}{c_d}\,\mathrm{e}^{c_d\pi\sigma}\right),$$

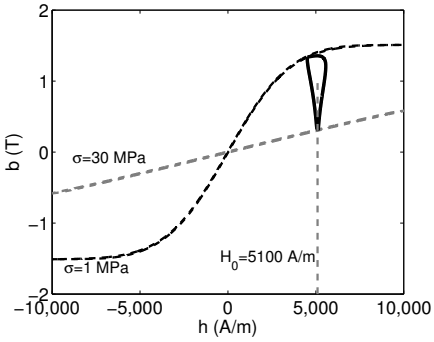

Figure 4: Projection of the periodic solution of system (2) on the (h, b) plane (solid bold line) for $\omega = 1$ Hz, $H_0 = 5100$ A/m, $R = 13\,\Omega$. Dashed curves show hysteresis loops such as in the upper panel of Figure 3(a) for fixed values of stress σ.

where $c = 0.48\,Am^{-1}$, $c_f = 3800$, $c_e = 280 \times 10^{-6}\,Pa^{-1}$, $c_a = -200 \times 10^{-6}\,Pa^{-1}$, $c_b = -0.32 \times 10^{-6}\,Pa^{-1}$, $c_c = 160 \times 10^{-6}\,Pa^{-1}$, $c_d = -0.14 \times 10^{-6}\,Pa^{-1}$, and

$$\psi(r, v) = \psi_0\big(\phi(v + r) - \phi(v - r)\big)\phi'(v + r)\phi'(v - r)$$

with

$$\psi_0(x) = c_0 \mathrm{e}^{-x/x_0}, \qquad \phi(x) = \tanh(ax + bx^3),$$

where ϕ' is the derivative of ϕ and $a = 0.58$, $b = 0.01$, $x_0 = 0.01$, $c_0 = 150.75\,V \cdot s/m^2$.

Remark that this choice is compatible with the hypothesis (50). Indeed, for $U > 0$,

$$\Psi_+ - k_+(U) = \int_0^\infty \int_{U-r}^\infty \psi(v, r)\,\mathrm{d}v\,\mathrm{d}r = \frac{1}{2}\int_U^\infty \int_0^y \psi_0\big(\phi(y) - \phi(x)\big)\phi'(y)\phi'(x)\,\mathrm{d}x\,\mathrm{d}y\,,$$

As ϕ increases, $\psi_0(\phi(y) - \phi(x)) \le c_0$, hence we obtain

$$\Psi_+ - k_+(U) \le \frac{c_0}{2}\int_U^\infty \int_0^y \phi'(y)\phi'(x)\,\mathrm{d}x\,\mathrm{d}y = \frac{c_0}{4}\big(\phi^2(\infty) - \phi^2(U)\big) \le \frac{c_0}{2}\,\mathrm{e}^{-2(aU+bU^3)},$$

which implies the first relationship in (50); the second relationship for $U < 0$ follows similarly.

Simulations of equation (2) with the above parameters and a piecewise linear periodic input $\sigma(t)$ oscillating between the values 1 MPa and 30 MPa were performed for two test frequencies of 1 Hz and 50 Hz of the input (see Figure 4). The electric load resistance R and the magnetic bias H_0 were used as control parameters. Note that, according to formulas (47), limits (52) can be realized by variation of these two parameters from zero to infinity.

Figure 5 presents the dependence of the output power (the harvested energy (3) normalized to the period of the input, E/T) on the parameters R, H_0. The power demonstrates a single maximum, which is quite sharp. The pick output power is higher for higher frequency of forcing.

In (2), the electric load of the harvester is modeled simply by a linear resistance, R. We have done simulations for a more complex model where the electric load also has a capacitance C, which is connected in parallel to the resistance R. The system is described by the equations

$$\frac{d}{dt}\left(\mu_0 h + \mathcal{P}\left[\frac{h}{f(\sigma)}, \lambda_{-1}\right]\right) = \frac{\ell r}{NS}\cdot(H_0 - h) - \frac{u}{NS} \tag{68}$$

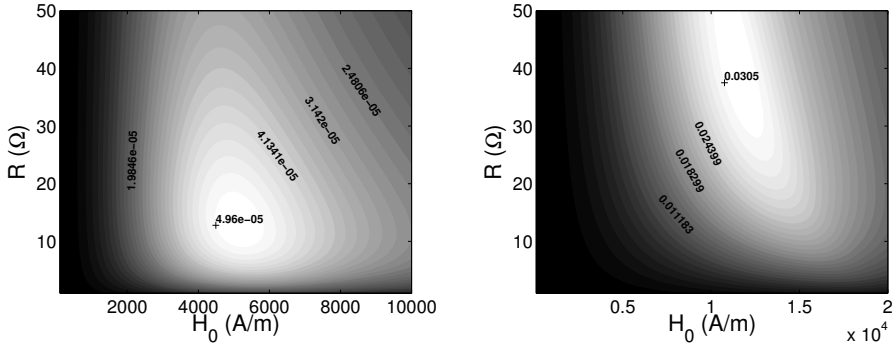

Figure 5: Dependence of the output power E/T (in the units of W) on the parameters R and H_0 shown by the intensity of gray color for the input frequency $\omega = 1$ Hz (a) and $\omega = 50$ Hz (b).

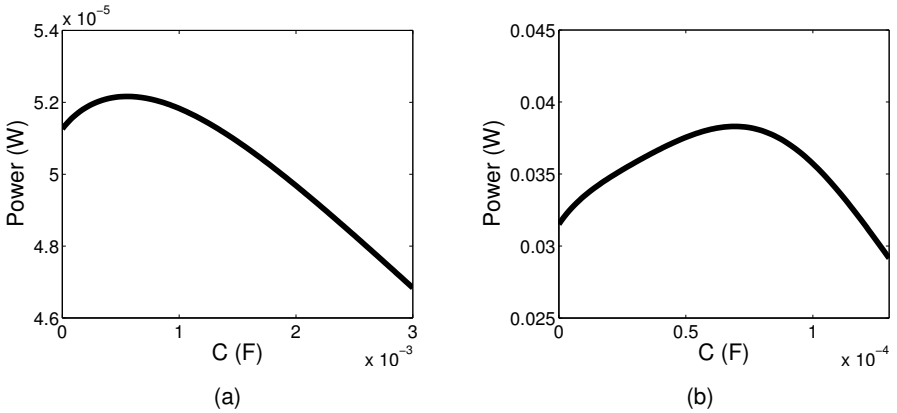

Figure 6: Dependence of the output power on the capacitance C for system (68), (69) for forcing σ with the frequency $\omega = 1$ Hz (a) and $\omega = 50$ Hz (b). The values of the parameters R and H_0 correspond to the peak output power of system (2) without the capacitor, see the corresponding panels of Figure 5. Other parameters are the same as in Figure 5.

$$\frac{du}{dt} = -\frac{\ell(H_0 - h)}{CN} - \frac{u}{CR} \tag{69}$$

where u is the drop of voltage across R (cf. (2)). Figure 6 presents the dependence of the output power on the capacitance C obtained by numerical simulation of this system. The maximum power is achieved for a positive value of C. The limit $C \to 0$ corresponds to system (2) without capacitance. Rigorous analysis of equations (68), (69) is a subject of future work.

References

[1] `http://www.iop.org/resources/energy/index.html`

[2] T. J. Kaźmierski and S. Beeby (eds.), *Energy Harvesting Systems*, Springer, 2011.

[3] S. R. Anton and H. A. Sodano, A review of power harvesting using piezoelectric materials (2003–2006), Smart Materials and Structures 16 (2007), R1.

[4] M. B. Moffett, A. E. Clark, M. Wun-Fogle, J. Linberg, J. P. Teter, and E. A. McLaughlin, Characterization of Terfenol-D for magnetostrictive transducers, The Journal of the Acoustical Society of America 89 (1991), 1448–1455.

[5] H. Ohta, S. W. Kim, Y. Mune, T. Mizoguchi, K. Nomura, S. Ohta, T. Nomura, Y. Nakanishi, Y. Ikuhara, M. Hirano, H. Hosono, and K. Koumoto, Giant thermoelectric Seebeck coefficient of a two-dimensional electron gas in SrTiO3, Nature Materials 6 (2007) 2, 129–134.

[6] G. D. Szarka, B. H. Stark, and S. G. Burrow, Review of power conditioning for kinetic energy harvesting systems, IEEE Transactions on Power Electronics 27 (2012) 2, 803–815.

[7] J. M. Renno, M. F. Daqaq, and D. J. Inman, On the optimal energy harvesting from a vibration source, Journal of Sound and Vibration 320 (2009), 386–405.

[8] S. Roundy, On the effectiveness of vibration-based energy harvesting, Journal of Intelligent Material Systems and Structures 16 (2005), 809–823.

[9] N. G. Stephen, On energy harvesting from ambient vibration, Journal of Sound and Vibration 293 (2006), 409–425.

[10] L. Wang and F. G. Yuan, Vibration energy harvesting by magnetostrictive material, Smart Materials and Structures 17 (2008), 045009.

[11] J. Hu, F. Xu, A. Q. Huang, and F. G Yuan, Optimal design of a vibration-based energy harvester using magnetostrictive material (MsM), Smart Materials and Structures 20 (2011) 1, 015021.

[12] A. H. Nayfeh, *Perturbation Methods*, John Wiley & Sons, 2004.

[13] A. Triplett and D. Quinn, The Effect of Non-linear Piezoelectric Coupling on Vibration-based Energy Harvesting, Journal of Intelligent Materials Systems and Structures 20 (2009) 16, 1959–1967.

[14] S. Stanton, A. Erturk, B. Mann and D. Inman, Nonlinear piezoelectricity in electroelastic energy harvesters: Modeling and experimental identification, J. Applied Physics 108 (2010), 074903.

[15] A. Erturk and D. J. Inman, *Piezoelectric Energy Harvesting*, John Wiley & Sons, 2011.

[16] A. Abdelkefi, A. H. Nayfeh, and M. R. Haj, Effects of nonlinear piezoelectric coupling on energy harvesters under direct excitation, Nonlinear Dynamics, 67 (2012) 2, 1221–1232.

[17] X. Dai, Y. Wen, P. Li, J. Yang, and X. Jiang, A vibration energy harvester using Magnetostrictive/Piezoelectric composite transducer, Proceedings of Sensors conference, IEEE (2009), 1447–1450.

[18] D. Davino, A. Giustiniani, and C. Visone, Magnetoelastic Energy Harvesting: Modeling and Experiments, in *Smart Actuation and Sensing Systems - Recent Advances and Future Challenges* (G. Berselli, R. Vertechy and G. Vassura, eds.), InTech, 2012, 487-512.

[19] C. Truesdell, *Rational Thermodynamics*, Springer Verlag, New York, 1984.

[20] A. Visintin, *Differential Models of Hysteresis*, Springer, 1994.

[21] F. Preisach, Über die magnetische Nachwirkung, Z. Physik 94 (1935), 277–302.

[22] A. Yu. Ishlinskii, Some applications of statistical methods to describing deformations of bodies, Izv. AN SSSR, Techn. Ser. 9 (1944), 583–590.

[23] L. Prandtl, Ein Gedankenmodell zur kinetischen Theorie der festen Körper, Z. Angew. Math. Mech. 8 (1928), 85–106.

[24] M. Ruderman and T. Bertram, Modified Maxwell-slip model of presliding friction, Proceedings of the 18th IFAC World Congress (2011), 10764–10769.

[25] M. Eleuteri, J. Kopfová, and P. Krejčí, A new phase field model for material fatigue in an oscillating elastoplastic beam, Discrete and Continuous Dynamical Systems - Series A 35 (2015) 6, 2465–2495.

[26] B. Appelbe, D. Flynn, H. McNamara, P. O'Kane, A. Pimenov, A. Pokrovskii, D. Rachinskii, and A. Zhezherun, Rate-independent hysteresis in terrestrial hydrology, IEEE Control Systems Magazine 21 (2009) 1, 44–69.

[27] P. Krejčí, J. P. O'Kane, A. Pokrovskii, and D. Rachinskii, Stability results for a soil model with singular hysteretic hydrology, Journal of Physics: Conference Series 268 (2011) 1, 012016.

[28] J. Peng and X. Chen, A Survey of Modeling and Control of Piezoelectric Actuators, Modern Mechanical Engineering 3 (2013) 1, 1–20.

[29] H. Haslach, Thermodynamically consistent, maximum dissipation, time-dependent models for non-equilibrium behavior, International Journal of Solids and Structures 46 (2009) 22-23, 3964–3976.

[30] D. Davino, P. Krejčí, and C. Visone, Fully coupled modeling of magneto-mechanical hysteresis through 'thermodynamic' compatibility, Smart Materials and Structures 22 (2013), 095009.

[31] P. Krejčí, *Hysteresis, Convexity and Dissipation in Hyperbolic Equations*, Gakkōtosho, Tokyo, 1996.

[32] M. Brokate, A. Pokrovskii, D. Rachinskii, and O. Rasskazov, Differential equations with hysteresis via a canonical example, in *The Science of Hysteresis* (I. Mayergoyz and G. Bertotti, eds.), vol. I, Elsevier, Academic Press, 2005, 125–291.

[33] M. Peigney and D. Siegert, Piezoelectric energy harvesting from traffic-induced bridge vibrations, Smart Materials and Structures 22 (2013) 9, 095019.

[34] H. J. Xiang, J. J. Wang, Z. F. Shi, and Z. W. Zhang, Theoretical analysis of piezoelectric energy harvesting from traffic induced deformation of pavements, Smart Materials and Structures 22 (2013) 9, 095024.

[35] P. Krejčí, On Maxwell equations with the Preisach hysteresis operator: the one-dimensional time-periodic case, Aplikace matematiky 34 (1989) 5, 364–374.

[36] M. Brokate and J. Sprekels, *Hysteresis and Phase Transitions*, Springer, New York, 1996.

[37] M. A. Krasnosel'skii and A. V. Pokrovskii, *Systems with Hysteresis*, Springer, 1989.

[38] M. Brokate, P. Krejčí, and D. Rachinskii, Some analytical properties of the multidimensional continuous Mroz model of plasticity, Control and Cybernetics 27 (1998) 2, 199–215.

[39] P. Krejčí, The Kurzweil integral and hysteresis, Journal of Physics: Conference Series 55 (2006), 144–155.

[40] M. Hilpert, On uniqueness for evolution problems with hysteresis, in *Mathematical Models for Phase Change Problems* (J. F. Rodrigues, ed.), Birkhäuser, Basel, 1989, 377–388.

[41] A. Pimenov and D. Rachinskii, Linear stability analysis of systems with Preisach memory, Discrete and Continuous Dynamical Systems B 11 (2009), 997–1018.

[42] A. Krasnosel'skii and D. Rachinskii, Bifurcation of forced periodic oscillations for equations with Preisach hysteresis, Journal of Physics: Conference Series 22 (2005) 1, 93–102.

[43] P. Krejčí, P. O'Kane, A. Pokrovskii, and D. Rachinskii, Properties of solutions to a class of differential models incorporating Preisach hysteresis operator, Physica D 241 (2012), 2010–2028.

[44] B. Kaltenbacher and P. Krejčí, A thermodynamically consistent phenomenological model for ferroelectric and ferroelastic hysteresis, ZAMM - Zeitschrift für Angewandte Mathematik und Mechanik, DOI: 10.1002/zamm.201400292.